

# Spin Index Determination of the Hawkeye Spacecraft

Scott A. Boardsen\* and Ramona L. Kessel†

NASA Goddard Space Flight Center, Greenbelt, Maryland 20770

We have developed a method to despin data from the Hawkeye spacecraft (1974–1978) that involves analyzing the variation of solar array voltage with sun phase angle. This new method is needed because the optical aspect system on the Hawkeye spacecraft failed four months into its mission, after which the spacecraft spin index could be determined only for limited periods using two other methods. Adding our new solar array technique nearly doubles the available data. The Hawkeye mission was designed to study high-latitude, high-altitude magnetosphere (exterior cusp, surrounding magnetopause and boundary layers, the polar cap, and Auroral field lines). The scientific payload was designed to measure the in situ plasma, magnetic, and electric fields. Besides Hawkeye, only the Highly Eccentric Orbiting Satellite-2 (HEOS-2) systematically explored this region of the Earth's geospace. Determining the spin index for the rest of the data, and subsequently despinning these data and representing them in a geophysically meaningful coordinate system, is still important due to the uniqueness of Hawkeye's orbit. The solar array method presented is based on searching parameter space for the solution that results in the best self-organization in spin index of the solar array voltage measurements. The spin index computed using this method is compared against the spin index determined from other methods. The resulting despun magnetic field data are compared with magnetic field models and with in situ magnetic field measurements in the solar wind made by the IMP-8 spacecraft.

## I. Introduction

ONLY two spacecraft, the Highly Eccentric Orbiting Satellite-2 (HEOS 2) and Hawkeye, have been launched into orbits that sample the high-latitude, high-altitude magnetosphere and magnetosheath on a routine basis. The HEOS 2 mission lasted for two years. Its magnetometer data are archived at a resolution of 32 s. Unfortunately, the rest of the data set, including the particle data, is lost. The NASA Langley Research Center/University of Iowa Hawkeye spacecraft was launched on 3 June 1974 and reentered on 28 April 1978. Its orbital period is  $\sim 51$  h, and its spin period is  $\sim 11$  s. Hawkeye's perigee is  $\sim 1.1 R_E$ , and its apogee is  $\sim 21 R_E$ . Its apogee is located above the northern hemisphere, making Hawkeye's orbit ideal for studying the high-latitude magnetopause and boundary layers around and antisunward of the northern cusp (Fig. 1). About 40 papers have been written using Hawkeye data, including far ranging topics such as the Earth as a radio source, electrostatic turbulence in the magnetosphere, plasma waves and instabilities in the polar cusp, the polarization and origin of auroral kilometric radiation, the auroral plasma cavity, high-latitude reconnection, and the exterior and interior polar cusps. All four years' worth of the original data, including engineering and trajectory data, have been preserved, but only about half of these were despun. Thus, important parameters such as the magnetic field direction and the plasma flow direction were not available for the undespun data. Despinning the rest of the Hawkeye data will almost double the amount of high-latitude data available to the scientific community. Current satellites such as the Defense Meteorological Satellite Program, POLAR, and Cluster-II do not sample this unique high-latitude region. In the foreseeable future, no missions will explore this region of geospace on a systematic basis.

To despin data measured by instruments on a spin-stabilized spacecraft such as Hawkeye, both the orientation of the spin axis

and a phase angle must be known. The phase angle is the angle in the spin plane measured, at a given time, from a reference point external to the spacecraft. For Hawkeye, this angle, which we call the spin index, is the angle in the spin plane between the sun direction projected into the spin plane and the positive  $x$  axis in the undespun spacecraft coordinate system, which is fixed relative to the spacecraft body. As the spacecraft rotates, this angle varies between 0 and 360 deg. The relation of the undespun spacecraft coordinate system to the spacecraft body is shown in Fig. 2. The spin axis is directed to a fixed point on the celestial sphere with a right ascension of  $299.4 \sim \text{deg} \pm 1.1 \text{ deg}$  and a declination of  $7.8 \sim \text{deg} \pm 1.5 \sim \text{deg}$  and varied little over the mission. The spin index was determined during the first four months using the optical aspect (OA) system, but on 3 September 1974, the system could not be commanded on after being turned off, and, therefore, the standard technique for despinning the data could not be further used.

After the failure of the OA system, a number of alternative methods were considered by Van Allen's group at the University of Iowa for determining the spin period and spin index (see Refs. 1 and 2). Two methods were developed and put into practice: One was to use the magnetometer,<sup>1</sup> and the other was to use the plasma instrument, a low-energy proton electron differential energy analyzer (LEPEDEA).<sup>2</sup> The magnetometer method compared the magnetic field measurements with a model magnetic field<sup>1</sup> and was applicable in regions where the magnetic field models are fairly reliable:  $> 200\gamma$  or  $< 5.4 R_E$  at low magnetic latitudes and  $< 6.8 R_E$  at high magnetic latitudes. However, only 10% of its orbit time was spent at radial distances less than  $< 6.8 R_E$ , and so the magnetometer method could be used only for a small portion of each orbit. The second method used the sun pulse detected by LEPEDEA.<sup>2</sup> This sun pulse was observed on a seasonal basis for about 80 days in the spring and 80 days in the fall. Therefore, about 160 calendar days per year could be despun using the LEPEDEA detected sun pulse. With the OA system and the two methods listed here, about 50% of the data were despun, leaving the other half undespun.

The approach we developed, which is based on solar array voltage measurements, to derive the spin index for the undespun half of the data set, is discussed in this paper. The reasons for using the solar array voltage is discussed in the next section, followed by a description of the despinning method that is centered on self-organization of solar array voltage measurements and their associated spin indices in voltage-index space. The development of a parameterized expression for the relative spin index is then discussed, followed by the application of this method. Finally, we discuss tests of accurateness and problems such as timing before giving conclusions.

Received 12 June 2001; revision received 5 March 2002; accepted for publication 11 March 2002. Copyright © 2002 by the American Institute of Aeronautics and Astronautics, Inc. No copyright is asserted in the United States under Title 17, U.S. Code. The U.S. Government has a royalty-free license to exercise all rights under the copyright claimed herein for Governmental purposes. All other rights are reserved by the copyright owner. Copies of this paper may be made for personal or internal use, on condition that the copier pay the \$10.00 per-copy fee to the Copyright Clearance Center, Inc., 222 Rosewood Drive, Danvers, MA 01923; include the code 0022-4650/02 \$10.00 in correspondence with the CCC.

\*Senior Scientist, Branch 632, L3 Communications Analytics Corporation (formerly Emergent Information Technologies, Inc.).

†Astrophysicist, Branch 632.

II. Why Solar Array Voltage Is Used for Despinning

For spin index determination, one wants a measurement that is sensitive to an external source of known location, like the sun, and whose response to this source varies periodically in a distinct manner as the spacecraft rotates. The contamination of the measurement from other sources must be small or removable. Because the solar array panel coverage on the spacecraft is asymmetrical about its spin axis, its instantaneous power output is periodic in a distinct manner. The response per spin is also approximately invariant over an orbit because of the constancy of the source, the large distance to the source, and the slow degradation of the panels in time. This invariance is only broken around perigee, where the Earth's albedo can make an ~20% contribution to the instantaneous power, and also in eclipse.

Thus, instantaneous solar array power is an ideal candidate for use in spin index determination, but, unfortunately, instantaneous solar array power is not sampled. However, the solar array voltage  $V$  is sampled. In Fig. 3a–3e, the solar array voltage (dots) minus its average value is plotted vs spin index for different 3-h segments along one orbit (except near perigee). The solid curve, which we call the spin modulation curve (SMC), is calculated by averaging all solar array voltage measurements (~1875) within  $\pm 24$  h of apogee into small angular bins in spin index and subtracting off the overall average. The voltage measurements trace out a similar distinct pattern in each panel, demonstrating that this measurement is periodic and

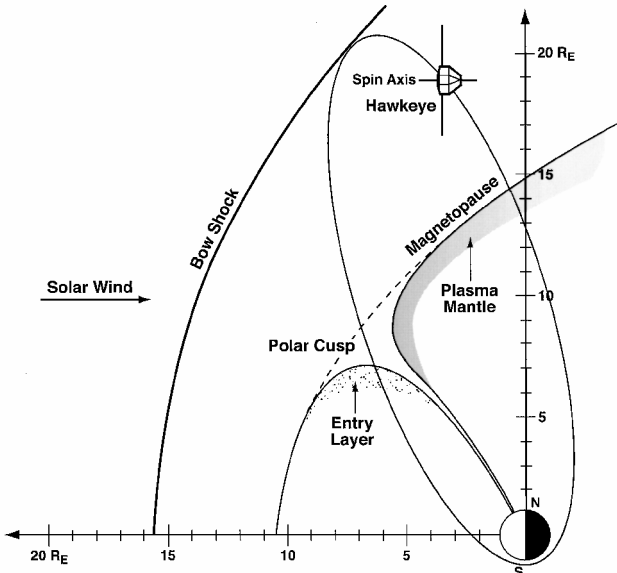


Fig. 1 Orbit of Hawkeye around the Earth.

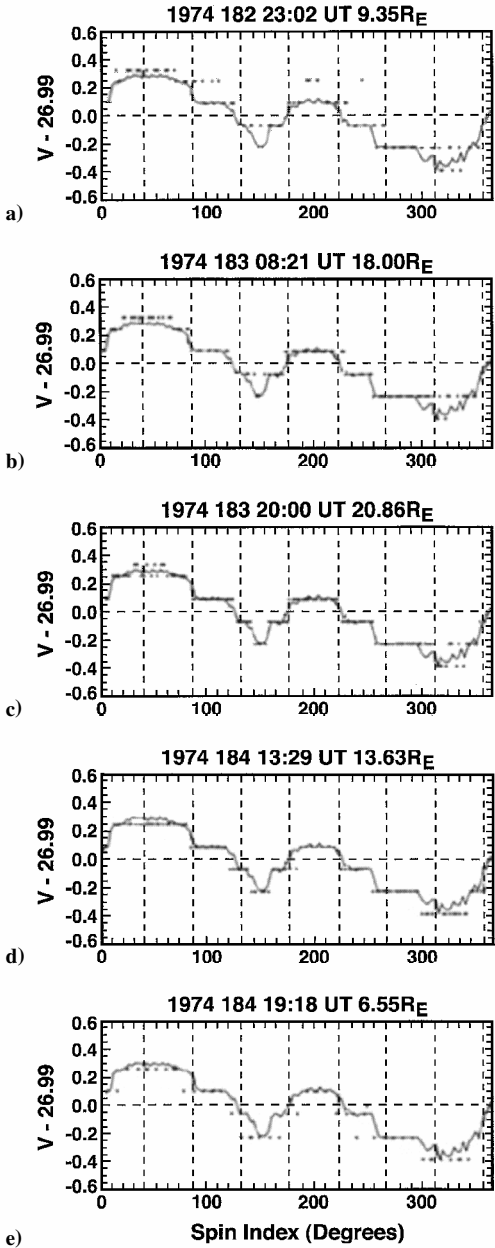


Fig. 3 SMCs for different orbital segments for a given orbit showing invariance of this curve throughout an orbit.

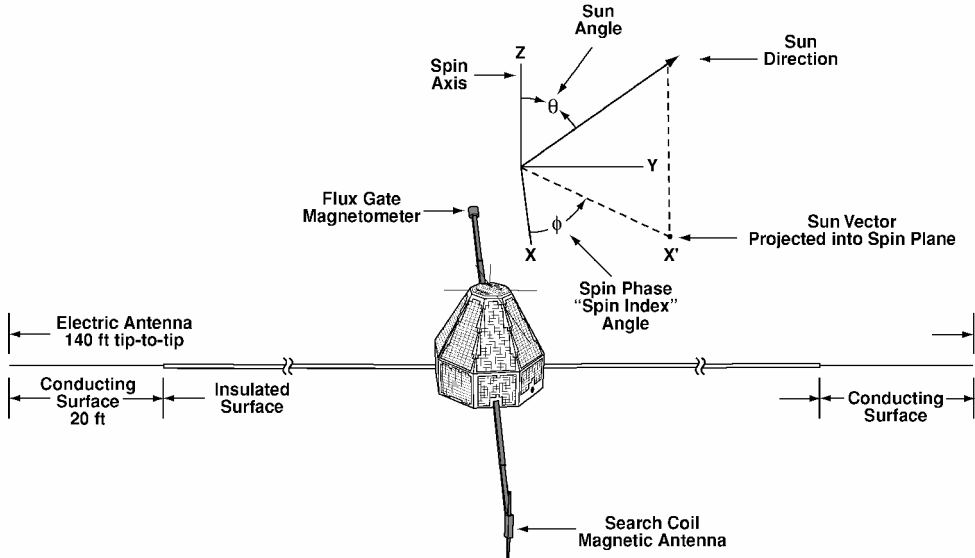


Fig. 2 Hawkeye spacecraft with undespun  $x$  and despun coordinate  $x'$  systems.

approximately invariant over the orbit, making this measurement a good candidate for use in spin index determination. We find this invariance to hold on all orbits tested.

Because the spacecraft's spin axis is not normal to the solar ecliptic plane, the solar illumination of the spacecraft changes slowly with calendar day as the sun angle changes [the angle between the spin (+Z) axis of the spacecraft and the sun direction; Fig. 2]. The sun angle varies from  $\sim 28$  deg on calendar day 24 to  $\sim 152$  deg on calendar day 207 each year. The shape of the pattern formed by the voltage measurements as a function of spin index is mainly determined by the sun angle as demonstrated in Figs. 4a–4f. The time at

apogee and the sun angle is given at the top of each of Figs. 4a–4f. The patterns and SMCs in Figs. 4c and 4d and Figs. 4e and 4f are very similar because they have similar sun angles, even though the measurements are made 365 days and 89 days apart, respectively. The octahedral shape of the spacecraft is apparent in Figs. 4e and 4f. We find that the shape of the SMCs as a function of sun angle is similar throughout the mission, and we will use this to compute calibration curves discussed in Sec. III.B.

### III. Description of the Despinning Method

If enough solar array voltage measurements are made so that the SMC is traced out per spacecraft rotation, then one could mark off this repeated pattern in a time series to despin the spacecraft. However, like most engineering data, this measurement is made infrequently, once every  $\sim 8.5$  spacecraft rotations. Therefore, another method is developed that relies on being able to model the instantaneous angular rotation rate of the spacecraft to high precision over a large time interval ( $\sim 48$  h covering  $\sim 16,000$  spacecraft rotations composed of  $\sim 1875$  voltage measurements). The high precision comes about by letting the data self-organize themselves in spin index as explained hereafter.

In principle, if the initial spin index  $\phi_0$  at time  $t_0$  and the instantaneous angular rotation rate  $\omega(t)$  is known over the time interval to be despun, then the spin index  $\phi(t)$  as a function of time  $t$  can be calculated from the following equation:

$$\phi(t) = [\phi_0 + \Delta\phi(t)] \bmod 2\pi \quad (1)$$

where  $\Delta\phi(t)$  is the relative spin index and is given by

$$\Delta\phi(t) = \int_{t_0}^t \omega(t') dt' \quad (2)$$

#### A. Determining $\Delta\phi(t)$ Through Self-Organization

The key for this method to work is that a parameterized expression  $\Delta\phi(t; \omega_0, \omega_1, \dots)$  must exist whose parameters  $\omega_0, \omega_1, \dots$  can be adjusted such that this expression becomes an accurate approximation to  $\Delta\phi(t)$  over the time range to be despun. If such an approximation cannot be found, this technique will not work. If such an approximation exists, then given a set of voltage measurements  $V_j$  taken at times  $t_j$ , relative phases  $\Delta\phi(t_j; \omega_0, \omega_1, \dots)$  can be assigned to these measurements. If the chosen parameters  $\omega_0, \omega_1, \dots$  result in a good solution for  $\Delta\phi(t)$ , the pattern formed by the set of points  $[V_j, \Delta\phi(t_j; \omega_0, \omega_1, \dots) \bmod 2\pi]$  will be distinct, with minimal scatter. If  $\omega_0, \omega_1, \dots$  results in a poor solution, then the pattern will be nondistinct with a lot of scatter.

We use the following expression to measure the amount of scatter in a pattern for a given  $\omega_0, \omega_1, \dots$ :

$$\kappa(\omega_0, \omega_1, \dots) = \frac{\sum_{i=1}^{n_B} m_i \sigma_i^2}{\sum_{i=1}^{n_B} m_i} \quad (3)$$

where

$$\sigma_i^2 = \sum_{j \in i} \frac{(V_j - \bar{V}_i)^2}{m_i} \quad (4)$$

$$\phi_{i-1} < [\Delta\phi(t_j; \omega_0, \omega_1, \dots) \bmod 2\pi] < \phi_i$$

$$\bar{V} = \sum_{j \in i} \frac{V_j}{m_i}, \quad \phi_{i-1} < [\Delta\phi(t_j; \omega_0, \omega_1, \dots) \bmod 2\pi] < \phi_i \quad (5)$$

The integer  $n_B$  is the number of evenly spaced bins between 0 and 360 deg into which the sensor measurements are sorted  $[\phi_i = 2\pi(i/n_B)]$ . The integer  $m_i$  is the number of measurements in bin  $i$ . The quantities  $\bar{V}_i$  and  $\sigma_i^2$  are the mean and variance of the sensor measurements in bin  $i$ . The weighted sum of  $\sigma_i^2$  yields the criteria for self-organization  $\kappa$ . If  $\omega_0, \omega_1, \dots$  yields a nondistinct pattern with a lot of scatter, then  $\kappa$  will be large. If  $\omega_0, \omega_1, \dots$  yields a distinct pattern with minimal scatter, then  $\kappa$  will be small.

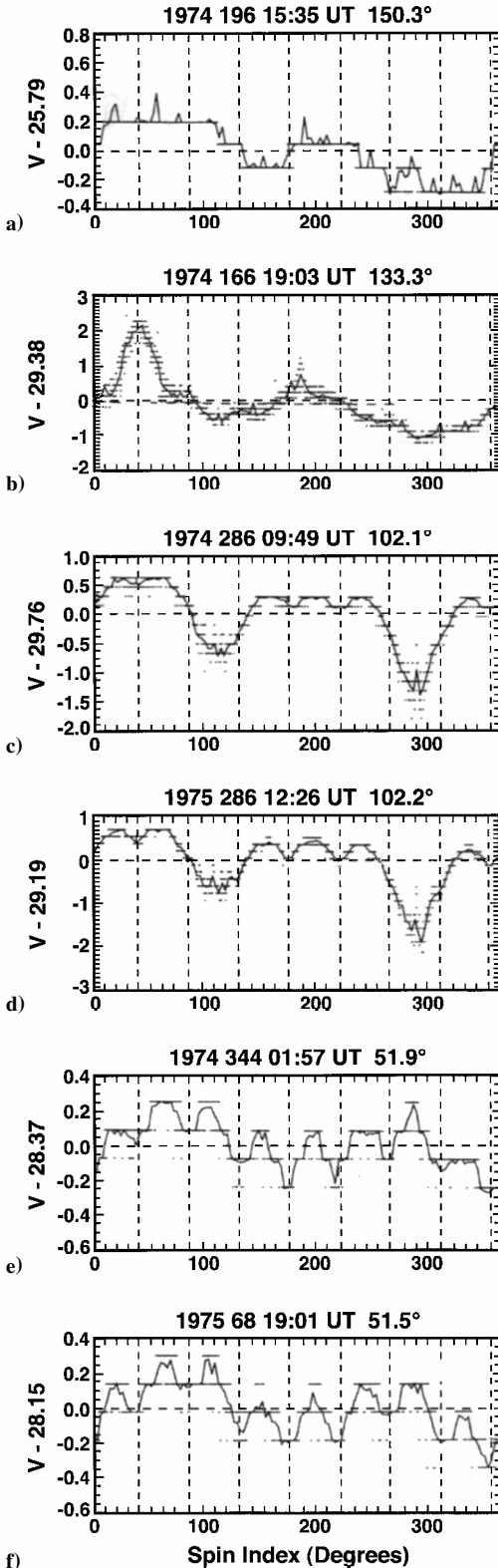


Fig. 4 SMCs for different sun angles (different times of year).

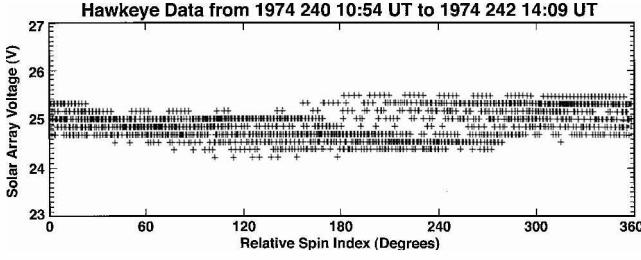


Fig. 5a Solar array voltage vs relative spin index before self-organization.

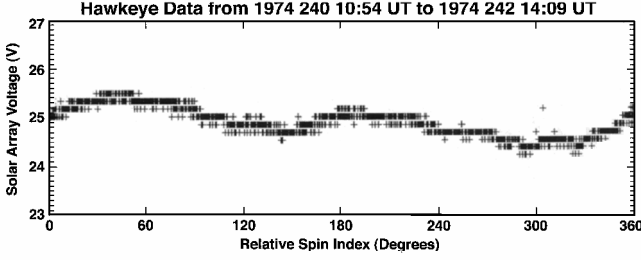


Fig. 5b Solar array voltage vs relative spin index after self-organization.

The  $\omega_0, \omega_1, \dots$  parameter space is searched until the global minimum is found whose resulting pattern does not exhibit aliasing (see Sec. IV.C). Figure 5a shows the pattern formed by plotting  $[V_j, \Delta\phi(t_j; \omega_0, \omega_1, \dots) \bmod 2\pi]$  using an initial guess for  $\omega_0, \omega_1, \dots$ . It is nondistinct with a lot of scatter. Figure 5b shows the pattern formed by the same measurements using  $\omega_0, \omega_1, \dots$  that were determined by finding the global minimum for  $\kappa$ . It is very distinct with minimal scatter.

The strength of this method is that prior knowledge of the pattern formed by the set of measurements is not needed to compute the relative spin indices, and many techniques can be developed to determine  $\phi_0$ . However, for this study, enough despun already data exist to determine the shape of these patterns such that calibration patterns (SMCs) can be derived and used to determine  $\phi_0$ .

### B. Determining $\phi_0$

To determine  $\phi_0$ , a set of calibration curves were generated from previously despun data (see Fig. 4 for examples). The sun angles of these curves cover the range from 40 to 152 deg. Unfortunately, no despun data are available for sun angles below 40 deg for generating calibration curves. The calibration curve whose sun angle is closest to the sun angle of the interval being despun is used for the determination of  $\phi_0$ . Determining  $\phi_0$  is done by computing  $\chi^2$ :

$$\chi^2 = \sum_{j=1}^m \frac{[V_j - V_{\text{cal}}[\phi(t_j)]]^2}{\sigma_{V_{\text{cal}}}[\phi(t_j)]^2} \quad (6)$$

for  $\phi_0$  spaced at 0.1-deg intervals from 0 to 360 deg and taking the global minimum as the solution, where

$$m = \sum_{i=1}^n m_i$$

is the total number of measurements,  $V_{\text{cal}}(\phi)$  is the calibration curve, and  $\sigma_{V_{\text{cal}}}(\phi)$  is the standard deviation of the calibration curves at spin index  $\phi$ .

### C. Approximation $\Delta\phi(t; \omega_0, \omega_1, \dots)$ for $\Delta\phi(t)$

As explained in Sec. III.A, it is crucial that a parameterized expression  $\Delta\phi(t; \omega_0, \omega_1, \dots)$  exists that is an accurate approximation to  $\Delta\phi(t)$  for a specific set of parameters  $\omega_0, \omega_1, \dots$  over the time interval to be despun. We find that the following approximation is sufficient:

$$\Delta\phi(t; \omega_0, \omega_1) = \omega_0 t + \frac{1}{2} \omega_1 t^2 \quad (7)$$

where  $\omega_0, \omega_1$  are the free parameters. Introducing higher-order terms in Eq. (7) did not result in better solutions for  $\Delta\phi(t)$ . Figure 6a shows the difference (solid jagged black trace) between the  $\Delta\phi(t)$  determined by the OA system and the least squares fit of Eq. (7) to the OA determined  $\Delta\phi(t)$  over one full orbit. Figure 6b shows the radial distance of the spacecraft. For the bulk of the orbit centered around apogee, we find that a set of values  $\omega_0, \omega_1$  can be determined such that Eq. (7) is a good approximation of  $\Delta\phi(t)$ . We find this to be true for all orbits despun using the OA system or sun pulse method and, therefore, conclude that this approximation is good for all orbits except around perigee or in eclipse. The deviation of the fit of Eq. (7) from the true solution when the spacecraft approaches perigee is due to thermal expansion/contraction of the spacecraft, primarily from the Earth's albedo and infrared radiation and/or when the spacecraft passes through the Earth's shadow.

The time derivative of  $\Delta\phi(t; \omega_0, \omega_1)$  gives the instantaneous angular frequency

$$\omega(t) = \omega_0 + \omega_1 t \quad (8)$$

From conservation of angular momentum, one expects this expression to be a constant when the spacecraft is at radial distances  $> 5 R_E$

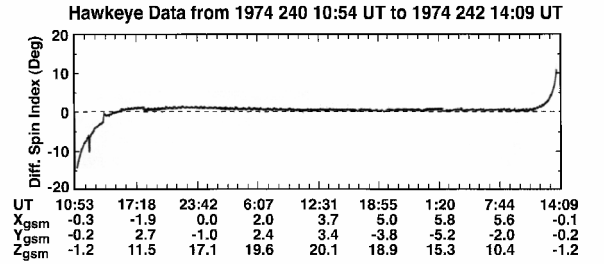


Fig. 6a Difference in spin index determined by the OA system minus the spin index determined by fitting Eq. (7) to the OA determined spin index.

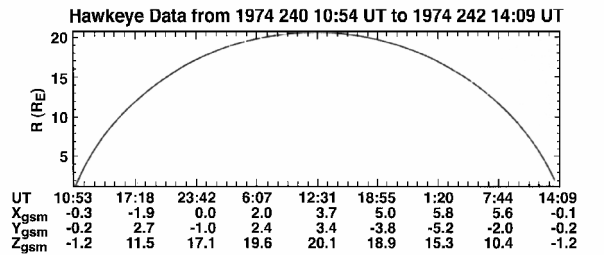


Fig. 6b Radial position of the spacecraft.

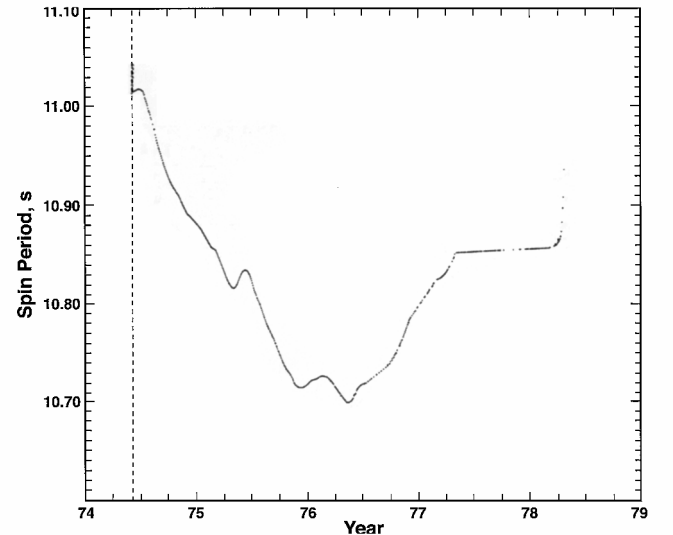


Fig. 7 Variation of the Hawkeye spin period throughout the four-year mission.

where the reflected and radiated energy flux from Earth becomes small, dropping off in intensity as  $\sim 1/r^{-2}$ . However, a term,  $\omega_1$ , linear in time, is necessary to model  $\omega(t)$  accurately over the orbit segment centered about apogee extending down to a few  $R_E$ . During the mission,  $|\omega_1/\omega_0| \leq 1.5 \times 10^{-9} \text{ s}^{-1}$ , with  $\omega_0 \sim 33 \text{ deg s}^{-1}$ . In general, the  $\omega_1$  term can not be dropped because the sparse sampling of the solar array voltages with time requires the despinning of large time intervals. Because we typically despin from at least a 24- to 48-h contiguous time interval, a drift error from  $<240$  to  $<720 \text{ deg}$  in the spin index solution can result if  $\omega_1$  is not included.

The variation of the spin period  $2\pi/\omega(t)$  over the mission is shown in Fig. 7. The spin period plotted in Fig. 7 is determined from the OA system or the LEPEDEA sun pulse or magnetometer methods of despinning the data. After the antennas' deployment and trim, an approximately linear 0.3-s decrease in spin period occurred over the first two years of the mission. The reason for the variation in the spin period has never been determined. We find the change to be uniform throughout the orbit, and so it is not due to effects around perigee, that is, frictional torque from the atmosphere or magnetic torque from the Earth's magnetic field.

#### IV. Applying the Despinning Method

The flowchart (Fig. 8) summarizes the procedure for despinning an orbit segment:

Step A) The orbit segment to be despun must be selected.

Step B) Then  $\kappa$  must be minimized.

Step C) The solution  $\omega_0, \omega_1$ , found by minimizing  $\kappa$ , is then checked for aliasing. If aliasing is found, modification of the initial guess or the orbit segment for despinning must be made and the process restarted at step B.

Step D) If the solution does not show aliasing, then  $\phi_0$  is determined, and the science data are despun and checked. If the despun

#### Goal: Despin Data by Solving for $\omega_0, \omega_1, \phi_1$ in Equations 1 and 7

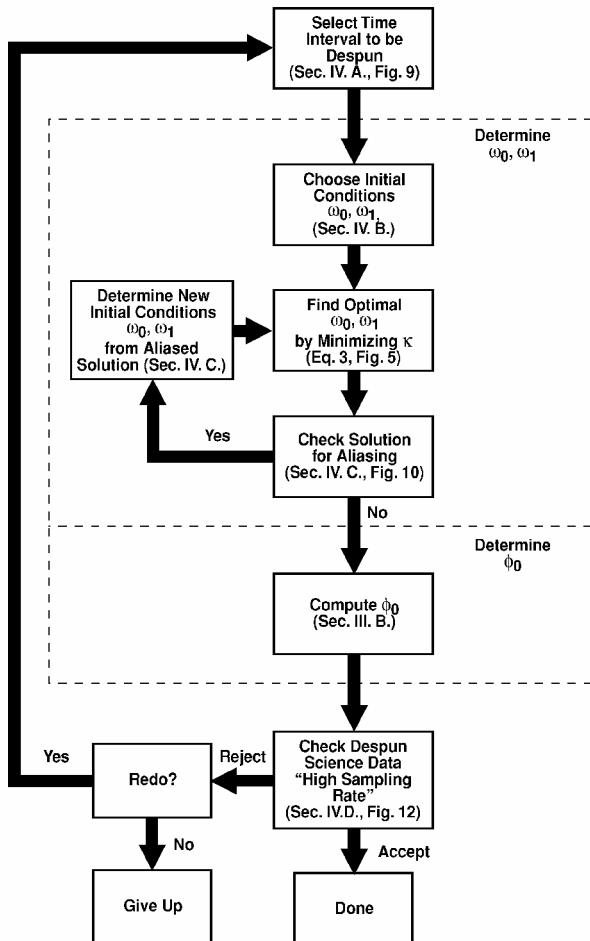


Fig. 8 Flowchart of steps in the despinning process.

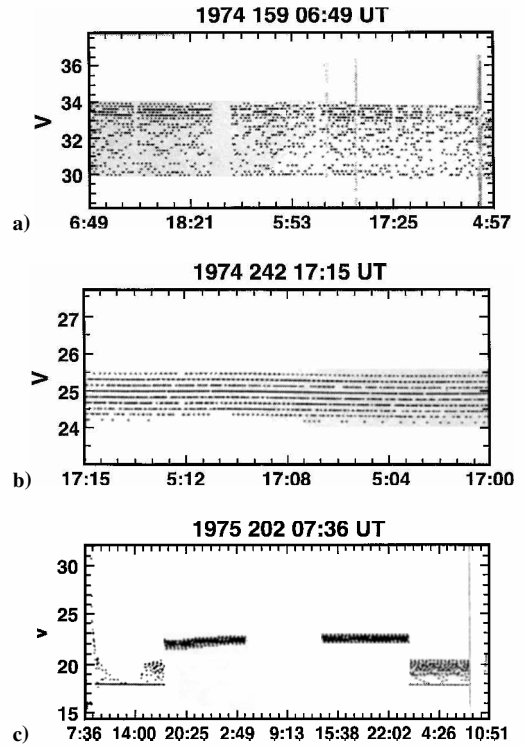


Fig. 9 Examples of different temporal variations in solar array voltage.

science data check out, the solution is accepted, if not the process is repeated after making adjustments. Each of these steps will be described in this section.

##### A. Step A: Choose the Time Interval

The following criteria are used to select the time interval over which to despin. Typically, the portion of an orbit was fitted where the radial position was greater than  $5R_E$ . No time interval contains either the perigee portion of the orbit or an eclipse period. This was because the spin index (phase angle) was difficult to model for these intervals. Figures 9a–9c show intervals of different temporal variations in the solar array voltage. The majority of the intervals were like those of Figs. 9a and 9b, in which the interval was despun as a whole. In general, we found that the greater the time interval the better the results. We typically despun a 24–48-h contiguous time interval at once. In Fig. 9c, a steplike transition in solar array voltage occurred. We found it best to break intervals like this into pieces and despin each piece separately. We suspect that the variations in Fig. 9c were due to changing power demands by the spacecraft.

##### B. Step B: Minimizing $\kappa(\omega_0, \omega_1)$

The simplex method of Nelder and Mead<sup>3</sup> (commonly called the amoeba method) is used to minimize  $\kappa$ . This method requires an initial guess for  $\omega_0, \omega_1$ , which is made by using the values from previously despun intervals that are closest in time. A scale length must be specified for  $\omega_0, \omega_1$ . The scale lengths were chosen by trial and error. Roughly, the amoeba takes steps in parameter space on the order of the scale lengths, adjusting the scale lengths as it goes along, until a minimum is found. (See Press et al.<sup>4</sup> for more details.) It is important that the initial scale length for  $\omega_0$  be large enough to reduce the likelihood of convergence on a minimum that is not global. This scale length must also be much smaller than the sampling frequency of the voltage measurements.

Before running the simplex method, the number of angular bins  $n_B$  used in the computation of  $\kappa$  must be determined. Because of the octahedral symmetry about the spacecraft's spin axis, many of the SMC curves exhibit octahedral symmetry, suggesting that the minimum number of bins should be 16, that is, a bin for each local minimum and maximum. From exploring the surface defined by  $\kappa$  in  $\omega_0, \omega_1$  space, it was determined that the depths of the local minimum are a function of  $n_B$ . The greater the number of bins, the deeper the

minima due to aliasing become, whereas the minima due to harmonics of the SMC become shallower. The true solution and its mirror solution and their  $|m| = 1$  aliases (Sec. IV.C) are the global minima of  $\kappa$ . These global minima were also found to have the largest widths in parameter space. By experimenting with  $n_B$  ranging from 4 to 128, we settled on  $n_B = 32$  for giving the best overall fit. By experimentation, we find that the number of voltage measurements must be greater than  $4n_B$ , and we are unable to obtain a good spin index solution if the time interval despun was less than 2 h, or 64 measurements distributed over 16 angular bins. Figure 5a shows the resulting (poorly organized) pattern in voltage measurements from the initial guess, and Fig. 5b shows the final (well-organized) pattern using the solution from the simplex method.

### C. Step C: Checking for Aliasing

Once a solution  $\omega_0, \omega_1$  is found by minimizing  $\kappa$ , the resulting pattern for this solution must be tested for aliasing because the angular sampling frequency  $\omega_s$  of 3.9 deg/s (sampling time  $t_s$  is 92.16 s) is much less than the angular spin frequency of  $\sim 33$  deg/s. We designate  $\omega_0^T, \omega_1^T$  as the true solutions for  $\omega_0, \omega_1$ . The true solution  $\omega_0^T$  can be written as

$$\omega_0^T = \omega_s(k + \alpha) \quad (9)$$

where

$$k = \text{fix}(\omega_0^T / \omega_s) \quad (10)$$

$$\alpha = (\omega_0^T / \omega_s) \text{ modulus } 1 \quad (11)$$

where  $0 \leq \alpha < 1$ . For Hawkeye,  $k = 8$  and  $0.37 < \alpha < 0.62$ . The relative phase for measurement  $i$ ,  $i = 0, n$  samples, taken at time  $it_s$  is

$$\begin{aligned} (\Delta\phi_i / 2\pi) \text{ modulus } 1 &= [(\omega_0^T / 2\pi) it_s + (\omega_1^T / 4\pi) i^2 t_s^2] \text{ modulus } 1 \\ &= (i\alpha + i^2\beta) \text{ modulus } 1 \end{aligned} \quad (12)$$

where  $\beta = (\omega_1^T / 4\pi) t_s^2$  and  $n^2\beta \leq 2$ . The pattern formed by the set of samples  $\{(\Delta\phi_i \text{ modulus } 2\pi), V_i; i = 0, n\}$  is independent of the integer value of  $k$ , and, therefore, different integer values for  $k$  represent alias solutions.

In general, alias solutions of the true solution are given by

$$\omega_{0ml} = \omega_s[l + \alpha]/m \quad (13a)$$

$$\omega_{1m} = \omega_1^T / m \quad (13b)$$

The quantities  $l$  and  $m$  are integers and  $m \neq 0$ . The integer  $|m|$  gives the number of times the pattern will be repeated between 0 and 360 deg. If  $m = 1$  and  $l = k$ , then Eq. (13a) becomes Eq. (9). If  $m = -1$  and  $l = -k - 1$ , then Eqs. (13a) and (13b) become

$$\omega_0^M = \omega_s[k + (1 - \alpha)] \quad (14a)$$

$$\omega_1^M = -\omega_1^T \quad (14b)$$

the pattern resulting from this solution is the mirror reflection about 180 deg of that of the true solution. The pattern, using simulated data, resulting from a true solution and its alias solution for  $m = 5$ , is shown in Fig. 10.

If the solution  $\omega_0, \omega_1$  showed  $m$  cycle aliasing in its pattern, the simplex routine was restarted using the following initial conditions for  $\omega'_0, \omega'_1$ :

$$\omega'_0 = \omega_s[k + (m\omega_0/\omega_s) \text{ mod } 1] \quad (15a)$$

$$\omega'_1 = m\omega_1 \quad (15b)$$

Equation (15a) is obtained by solving Eq. (13a) for  $\alpha$  and substituting it into Eq. (9).

Having found a solution where  $|m| = 1$ , it must then be determined whether this solution is the true solution equation (9) or the mirror solution equation (14). For Hawkeye, determining which solution to

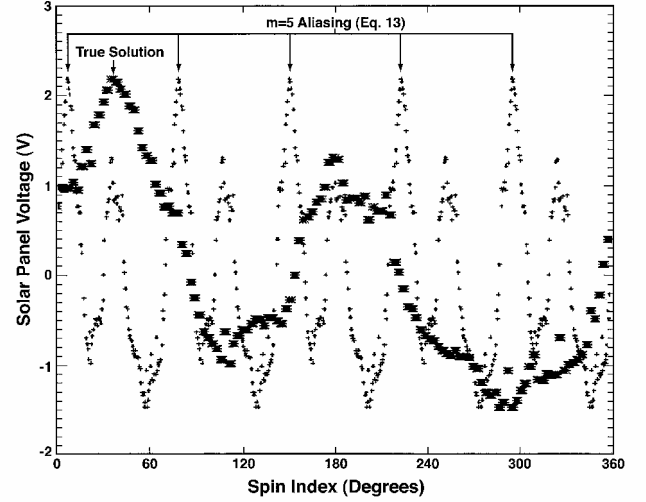


Fig. 10 Simulated data showing SMC for true solution (large dots) and for  $m = 5$  aliasing (small dots).

choose is generally not a problem because the maximum change in  $\omega_0$  between consecutive orbits ( $< 0.009$  deg/s) is much less than the separation between the true solution and mirror solution  $\omega_s(2 - \alpha)$  for most of the mission. Thus, if the solution from a neighboring orbit is known, then the correct solution can be determined as long as the following condition holds:

$$|0.5 - \alpha| > \Delta\omega_0/\omega_s \sim 0.0023 \quad (16)$$

However, when this condition is violated, that is, when  $\alpha$  goes through 0.5, a resonance, then earlier knowledge of the spin index curve is used for similar sun angles in choosing the correct solution. Magnetometer data are also used, because their angular sampling frequency of 180 deg/s is much greater than  $\omega_s$ . (See Sec. IV.D on how magnetometer data are used.) If the solution was found to be the mirror solution, then

$$\omega'_0 = \omega_s\{k + [1 - (\omega_0/\omega_s) \text{ mod } 1]\} \quad (17a)$$

$$\omega'_1 = -\omega_1 \quad (17b)$$

were used as initial conditions in reminimizing  $\kappa$ .

Resonances occur whenever

$$\alpha = m_1/m_2 \quad (18)$$

where  $m_2 > m_1$  are positive integers composed of no common factors. Exactly at a resonance, the solar array voltage is sampled at only  $m_2$  discrete points in spin index. For Hawkeye, the  $\omega_1$  term varies enough over an orbit segment that going through a resonance is not a problem because the solar array voltages are sampled over the entire range of spin index.

Besides alias solutions contributing local minimum to  $\kappa(\omega_0, \omega_1)$ , harmonics of the Fourier transform of the spin index curve can also contribute to a local minimum. For example, the second harmonic of the Fourier transform of the spin index curve in Fig. 10 is twice as large as that of the fundamental. In this situation, trial and error is heavily relied on in changing the initial guess for reminimizing  $\kappa$ . However, if the harmonic number  $m_3$  associated with minimal  $\kappa$  can be identified, one can try

$$\omega'_0 = \omega_s[k + [1 - (\omega_0/m_3\omega_s) \text{ mod } 1]] \quad (19a)$$

$$\omega'_1 = \omega_1/m_3 \quad (19b)$$

as a new initial guess.

After determining  $\omega_0, \omega_1$ , then  $\phi_0$  is determined using the method described in Sec. III.B.

To test the reliability and accuracy of this method, it was tested on 102 orbits that were already despun by either the OA system or the LEPDEA sun pulse method. Because we cannot despin

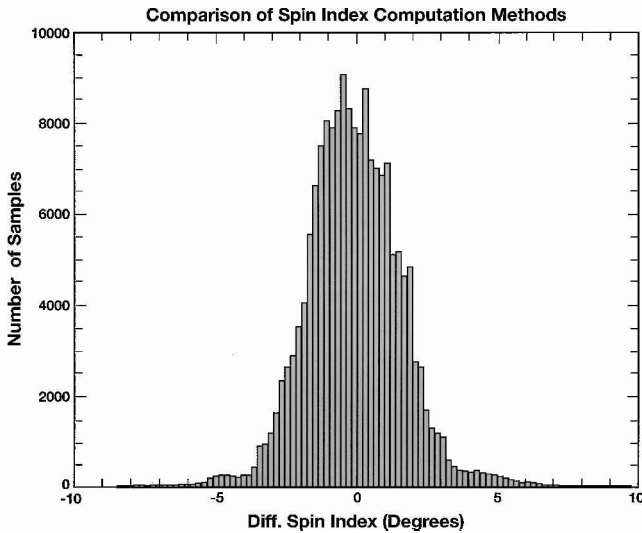


Fig. 11 Distribution in the error in the spin index solution using the solar array method.

through perigee, this method was applied to each orbit separately over a  $\sim 48$ -h time interval centered around the apogee of each orbit. The distribution of the difference between the spin index solution using this method and either the OA solution or the LEPDEA sun pulse solution is shown in Fig. 11. This distribution is composed of 172,395 measurements from these 102 orbits. The standard deviation of this distribution is  $\sim 2$  deg about a mean of 0 deg. Based on this distribution, the error in determining the spin index solution is estimated to be less than 5 deg 98% of the time, less than 2 deg 80% of the time, and less than 1 deg 46% of the time.

#### D. Checking Despun Science Data

In applying this method to previously undespun intervals, visual checks are used to gauge the reliability of the spin index solutions. To do this, the despun Hawkeye magnetometer data are compared with the Tsyganenko and Stern magnetic field model<sup>5</sup> and with near-Earth interplanetary magnetic field (IMF) measurements. The IMF measurements were made by Interplanetary Monitoring Platform-8 (IMP-8) ( $\sim 33 R_E$  semicircular midlatitude orbit about Earth) when it was in the solar wind. The Tsyganenko and Stern model is applicable inside the Earth's magnetosphere; the despun magnetometer data should be in reasonable agreement with those of the Tsyganenko and Stern model when Hawkeye is in the magnetosphere. Because the solar wind near Earth is approximately homogeneous, the IMF direction and the Hawkeye magnetic field direction should be in reasonable agreement when Hawkeye is in the solar wind. These measurements should be in rough agreement when Hawkeye is in the magnetosheath, where it detects the shocked solar wind after passage through the Earth's bow shock.

Figure 12 is an example of the plot we developed to help detect any gross errors that occurred in the spin index solution. Solutions were not extrapolated through perigee. In Figs. 12a–12c, the black traces (dots) are despun Hawkeye magnetometer measurements, whereas the red trace is the Tsyganenko and Stern<sup>5</sup> model, and the green dots are 5-min resolution IMP-8 IMF measurements while in the solar wind. Figure 12a displays the magnetic field magnitudes, Fig. 12b displays the latitudinal angle in geomagnetic solar magnetospheric coordinates (GSM) of the magnetic field direction, and Fig. 12c displays the  $\phi$  angle in GSM of the magnetic field direction.

For this example, Hawkeye was in the magnetosheath from day 349,  $\sim 2000$  universal time (UT) to day 350,  $\sim 1330$  UT, and on day 350 from  $\sim 1930$  UT to  $\sim 2300$  UT. For these time periods, the Hawkeye magnetic field directions are in reasonable agreement with the IMF directions. The plasma flow direction in the magnetosheath is steadier than the sheath magnetic field direction, tending to flow tailward. It is plotted as black dots in Fig. 12d. The smooth purple curve shows the estimated flow direction based on a simple steady-state model of the magnetosheath flow direction. In the magnetosheath, a sharp break in this flow direction not accompanied by

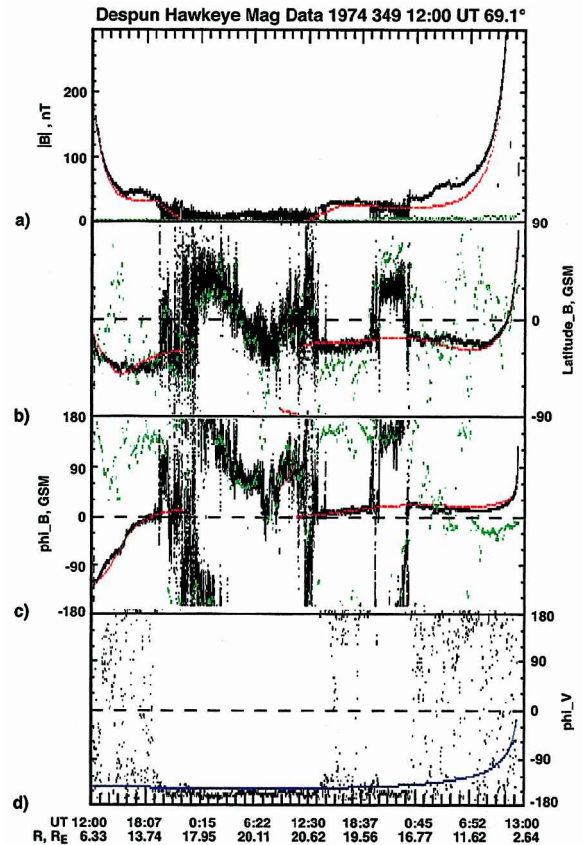


Fig. 12 Example survey plot used to judge the reliability of the spin index solution is shown; comparison of despun magnetic field and flow direction to models.

a sharp change in the solar wind direction would indicate a potential error in the spin index solution. For times in Fig. 12 outside of these two intervals, Hawkeye is in the magnetosphere, and the Hawkeye magnetic field directions are in reasonable agreement with the directions computed from the Tsyganenko and Stern<sup>5</sup> model. This agreement indicates that the despun solution for this orbit is reasonable and contains no gross errors. Because the magnetometer data have a high sampling rate, errors in despinning, like aliasing, will show up as oscillations in the magnetic field direction (Figs. 12b and 12c) when Hawkeye is inside the magnetosphere.

For the survey plots (see Fig. 12 for an example), an error of  $> 5$  deg is easy to pick up when Hawkeye is in the magnetosphere because a noticeable discontinuity in the magnetic direction traces is present (Figs. 12c and 12d). To judge the reasonableness of the spin index solutions, plots like these were generated for the entire Hawkeye mission and visually inspected. For intervals in which the solution seemed unreasonable, the spin index solution for that interval was recomputed after making adjustments. These adjustments involve changing  $n_B$ , making small modifications to the initial guesses and/or subdividing the interval into subintervals, and fitting each subinterval separately.

#### V. Discussion

The method described in this paper can be potentially applied to other spacecraft (spinors or dual spinors) that have experienced attitude system failures if items 1–5 in the following list are satisfied:

- 1) A sensor measurement must be available whose response to an external source of known location is distinct and periodic with respect to the spacecraft's spin period and is invariant over the interval to be despun.
- 2) A good parameterized approximation such as Eq. (7) and demonstrated in Fig. 6a, must exist for the relative phase [Eq. (2)].
- 3) A method for determining  $\phi_0$  must be developed.
- 4) If the data are sampled at a rate of less than half of the spin period, a method must be developed to remove aliasing from the solution.

5) The spin axis orientation must be known.

Items 6–9 are useful in support of the first five items.

6) Science-quality vector magnetometer measurements with a sampling rate greater than half of the spin period are desirable.

7) The availability of despun data, before the failure of the spacecraft attitude system, that can be used to test the reliability of this method is desirable.

8) Preflight calibration data of the sensor response for different spacecraft orientations with respect to the sun is desirable (not available for Hawkeye).

9) A preflight model of the sensor response (not available for Hawkeye) is desirable.

Item 1 is the most critical; for Hawkeye the solar array voltage measurements best satisfy this item as demonstrated in Fig. 3. For Hawkeye, item 7 was satisfied and used for determining  $\phi_0$  (item 3), as explained in Sec. III.B. However, if item 7 is not satisfied, magnetometer measurements (item 6), if available, can be used in regions where magnetic field models are reliable to determine item 3. They can also be used to determine items 4 and 5. The function [Eq. (3)] we use to measure the degree of self-organization relies on the SMC being single valued as a function of spin index. If this is violated, a more complicated measure must be developed. For example, if an instrument was drawing large amounts power, in a cycle, from the spacecraft, this could cause the pattern formed by the voltage measurements to be double valued as a function of spin index, requiring a different and computationally more taxing measure than the one used in this study.

One problem to be aware of is the potential existence of timing errors in the sensor measurement time tag. For Hawkeye, a 1-s error would lead to a  $\sim 33$ -deg error in the spin index solution for data despun during that interval. This method is dependent on the relative time being sufficiently linear over the interval for which the spin index solution is being determined. We suspect that the two potential sources of timing errors are 1) radiation upsetting the spacecraft clock and 2) conversion from spacecraft time to universal time on the ground. We suspect that case 2 happened occasionally when spacecraft tracking was switched to a different ground station.

## VI. Summary

In summary, the method developed in this paper was successfully applied in determining the spin index of the Hawkeye spacecraft.

This method relies on self-organization of the solar array voltage measurements in the spin index. Orbit data previously undespun over the mission were despun in this study, excluding the orbit segments around perigee due to thermal expansion and the effects of albedo. Based on comparing this method with other methods for spin index determination, it is estimated that the accuracy of this method is about  $\sim 2$  deg. The resulting despun magnetometer data for the entire Hawkeye mission have been converted to the scientific common data format and archived at the National Space Science Data Center (NSSDC). The data set is presently available via the Coordinated Data Analysis Web (CDAWeb) for plotting and/or downloading files (<http://cdaweb.gsfc.nasa.gov>). The despun check plots (see Fig. 12 for an example) are also presently electronically accessible via the Hawkeye Web page at NSSDC (<http://nssdc.gsfc.nasa.gov/hawkeye/hawkeye.html>).

## Acknowledgments

This data restoration project was supported by NASA Goddard Space Flight Center Grant 370-03-00-11. We would like to thank J. A. Van Allen at the University of Iowa for his help and useful comments and for supplying us with his project memorandums. We would also like to thank J. L. Green at the National Space Science Data Center for his support and useful suggestions.

## References

- <sup>1</sup>Chen, T.-F., "The Earth's Magnetic Field at Large Radial Distances as Observed by Hawkeye 1, M.S. Thesis, Dept. of Physics and Astronomy, Univ. of Iowa, Iowa City, IA, May 1978.
- <sup>2</sup>"Hawkeye 1/Neutral Point Explorer," Dept. of Physics and Astronomy, Final Rept., Univ. of Iowa, Iowa City, IA, March 1977.
- <sup>3</sup>Nelder, J. A., and Mead, R., "A Simplex Method for Function Minimization," *Computer Journal*, Vol. 7, No. 4, 1965, pp. 308–313.
- <sup>4</sup>Press, W. H., Flannery, B. P., Teukolsky, S. A., and Vetterling, W. T., *Numerical Recipes, the Art of Scientific Computing*, Cambridge Univ. Press, Cambridge, MA, 1991, p. 295.
- <sup>5</sup>Tsyganenko, N. A., and Stern, D. P., "Modeling the Global Magnetic Field of the Large-Scale Birkeland Current Systems, *Journal of Geophysical Research*, Vol. 101, No. A12, 1996, pp. 27,187–27,198.

A. C. Tribble  
Associate Editor

Color reproduction courtesy of NASA Goddard Space Flight Center.